

## CHEMICAL CHANGES OF TITANIUM AND TITANIUM DIOXIDE UNDER ELECTRON BOMBARDMENT

R. Brasca<sup>1</sup>, L.I. Vergara<sup>2,a</sup>, M.C.G. Passeggi (Jr.)<sup>2,\*</sup> and J. Ferrón<sup>1,2</sup>

\* INTEC (CONICET-UNL), Güemes 3450, (S3000GLN) Santa Fe, Argentina,  
mpggih@intec.unl.edu.ar

1.- Facultad de Ingeniería Química, Universidad Nacional del Litoral, Santa Fe, Argentina

2.- Laboratorio de Superficies e Interfaces, Instituto de Desarrollo Tecnológico para la Industria Química, INTEC (CONICET-UNL), Santa Fe, Argentina

### ABSTRACT

*The electron induced effect on the first stages of the titanium oxidation and titanium dioxide ( $Ti^{4+}$ ) chemical reduction processes have been studied by means of Auger electron spectroscopy. Using Factor Analysis we found that both processes are characterized by the appearance of a lower Ti oxidation state,  $Ti_2O_3$  ( $Ti^{3+}$ ).*

Keywords: Titanium, Titanium oxides, AES, electron bombardment, Factor Analysis

### INTRODUCTION

Thin metal oxide films over metal and semiconductor surfaces are probably the most widely studied structures in basic physics and technology. The reason is quite simple; their applications cover areas of interest such as catalysis<sup>(1)</sup> microelectronic devices<sup>(2,3)</sup>, medicine<sup>(4,5)</sup>, and aircraft construction<sup>(6)</sup>. Metal-metal oxide structures involving titanium (Ti) are among the most interesting and used ones. Thus, the surface oxide passivation of Ti makes possible the biocompatibility of Ti and its use in medicine, and the production of protective coatings against corrosion<sup>(7)</sup>. Since most of the useful properties are determined by phenomena occurring at the surface, the kinetic and thermodynamic features of the oxide films growth and chemical reactions at the surfaces are key facts in most of these processes. These chemical reactions can be greatly affected by the incidence of energetic particles or photons.

---

<sup>a</sup> Present address: Dept. of Chemistry, University of Tennessee, Knoxville, TN 37996 USA.

While sometimes these reactions are looked for wanted effects, such as in electron lithography<sup>(8-10)</sup>, in other cases they represent experimental artifacts, like in surface analysis techniques based on electron spectroscopies. The chemical reactions can be either oxidation or reduction depending on the particular substrate. Thus, while in electron lithography the desired effect is the metallic reduction<sup>(11)</sup>, the electron bombardment can enhance by several orders of magnitude the oxidation kinetic of a semiconductor<sup>(12,13)</sup>. The identification of the different products appearing in the growth of oxide films, as well as in the different reaction occurring at surfaces, allows us a better understanding of the different processes and, at the same time, opens the possibility of designing reliable growth and characterization methods.

In this paper, using Auger electron spectroscopy (AES) and Factor Analysis (FA)<sup>(14)</sup>, applied in the sequential way<sup>(15,16)</sup>, we study the oxidation process of metallic titanium and the reduction process of a TiO<sub>2</sub> thin film under electron irradiation. In both cases we determine the chemical state of the different compounds formed over the surface. The application of FA to the Auger spectra allows us to obtain the spectra of the different species formed along the irradiation process.

## EXPERIMENTAL DETAILS

### EXPERIMENTAL SETUP

All measurements were performed at room temperature in a commercial ultra high vacuum (UHV) surface analysis system with a base pressure in the lower 10<sup>-10</sup> Torr range, equipped with Auger electron spectroscopy (AES) facilities. Differentiated Auger spectra of the transitions Ti<sub>LMM</sub>, Ti<sub>LMV</sub> and O<sub>KLL</sub> were acquired using a single-pass cylindrical mirror analyzer with a resolution of 0.6 % and modulation amplitude of 4 and 2 V<sub>p-p</sub> for the oxidation and reduction processes, respectively. The incidence angle of the electron beam was 30° with respect to the surface normal. The primary electron beam energy was 3 keV, the irradiated area ~ 7×10<sup>-5</sup> cm<sup>2</sup>, the electron gun was permanently switched on during the oxidation and reduction processes, and the acquisition of the Auger spectra was performed within the same irradiation conditions. The current density was 48 and 30 mA/cm<sup>2</sup>, for the oxidation and reduction processes, respectively.

The sample used for the oxidation process was high-purity polycrystalline titanium (with 125 ppm of impurities including Fe, Si, Mn, Mg and Sn). The sample

surface was cleaned by ion bombardment using  $\text{Ar}^+$  at 4 keV until carbon and oxygen contamination was below the AES detection limits. The UHV chamber was filled with high purity oxygen (better than 99.997 %) at a pressure of  $2 \times 10^{-8}$  Torr. The pressure was measured by means of a non-corrected Bayard-Alpert gauge and the oxygen exposure was maintained at least until the saturation of the oxygen Auger signal was obtained.

The  $\text{TiO}_2$  film for the reduction process was grown over a Cu(100) single crystal, cleaned by cycles of  $\text{Ar}^+$  ion bombardment (1 keV) followed by annealing at 850 K, until carbon and oxygen contamination was below the AES detection limit. The  $\text{TiO}_2$  film was prepared by Ti thermal evaporation from a high purity polycrystalline Ti bar heated through electron bombardment in an  $\text{O}_2$  environment ( $2 \times 10^{-7}$  Torr). The Cu substrate was kept at room temperature during the co-adsorption process, which leads to the formation of stoichiometric amorphous  $\text{TiO}_2$  films with an abrupt interface with the Cu substrate <sup>(17)</sup>. The evaporation rate was determined through the attenuation of the substrate signal with deposition time, being a typical value 0.15 ML/min. The analyzed films were  $\sim 10$  ML thick. This thickness was large enough to attenuate any Auger signal coming from the substrate, but small enough to prevent sample charging.

The irradiation dose  $\phi$  was calculated as  $\phi = J_a \cdot t_i$ , where  $J_a$  is the current density and  $t_i$  the total irradiation time in seconds. Since, the same irradiation conditions were used during the AES spectra acquisition, the total dose was obtained by the addition of irradiation and acquisition times. A typical spectrum acquisition time was 30 seconds and the whole irradiation time until saturation  $\sim 6$  hours.

### DATA TREATMENT

The Factor Analysis (FA) method <sup>(14)</sup> has been extensively discussed in previous works <sup>(12,15,16,18,19)</sup>, and it is currently included as a standard data treatment system in most data treatment packages. Therefore we will limit ourselves here to a brief description. The first step in FA is the determination of the number of linearly independent factors, i.e. the minimum number of pure components required to describe the complete series of spectra corresponding to the evolution under study. In doing that, we compare the error obtained, by fitting the experimental data with a minimum set of factors, with the experimental error (EE). This procedure is performed

as Auger spectra are added in a sequential way <sup>(15)</sup>, and each time the fitting error surpasses the experimental one, a new factor appears in the process.

Once the number of independent factors is known, the Auger line shape of each pure component (or base) is determined through a least square fit procedure called Target Transformation (TT) <sup>(14,15)</sup>. The final step in FA is the correlation among the obtained bases and actual compounds, which is performed through a simple fingerprint procedure. Since the experimental Auger spectra of all Ti compounds involved in this study are available in the literature <sup>(19-24)</sup>, this final step is easily performed.

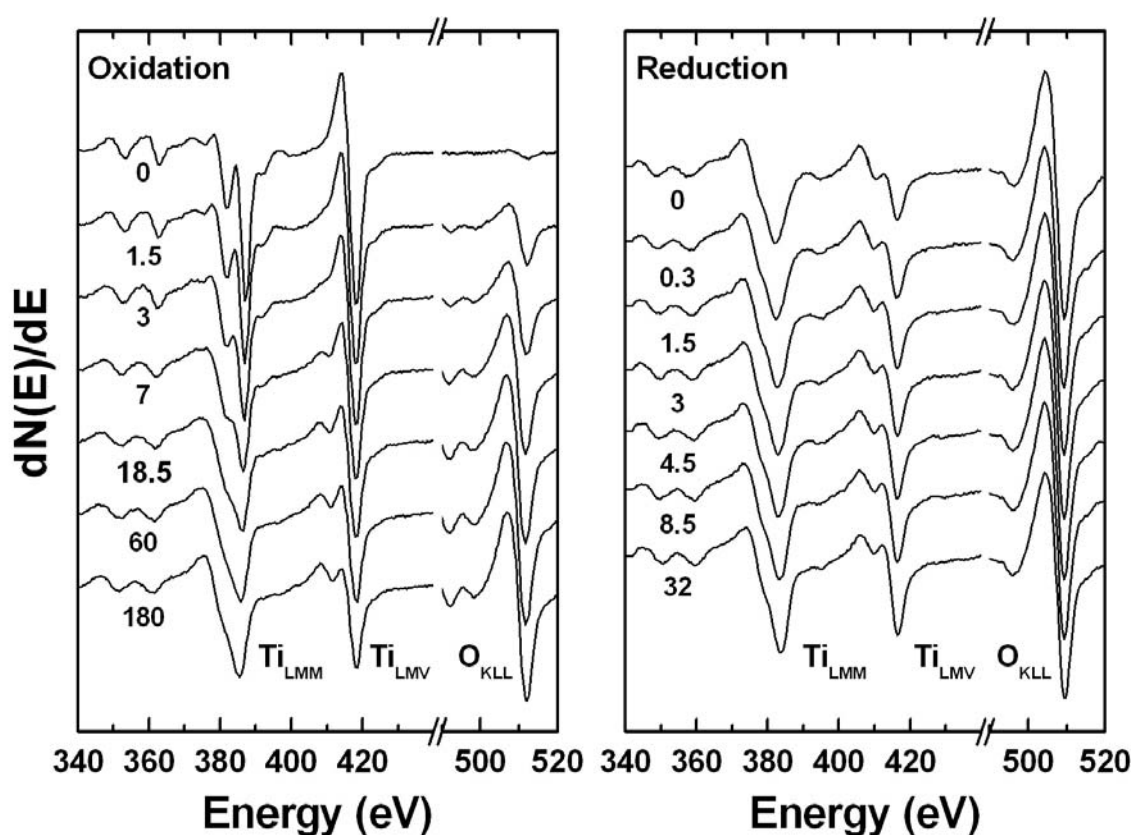


**Figure 1:** Ti<sub>LMM</sub> (340-395 eV), Ti<sub>LMV</sub> (395-440 eV) and O<sub>KLL</sub> (490-520 eV) Auger line shapes evolution during the electron stimulated oxidation of metallic Ti (left panel) and reduction of a TiO<sub>2</sub> film under electron irradiation (right panel).

## RESULTS AND DISCUSSION

In figure 1 we present two sets of spectra showing the evolution of the Auger line shape corresponding to the Ti<sub>LMM</sub>, Ti<sub>LMV</sub> and O<sub>KLL</sub> transitions as a function of the electron irradiation time during the Ti oxidation (left panel) and TiO<sub>2</sub> reduction (right panel) processes. As the bombardment time increases, the spectra show the

growth/decrease of the amount of oxygen at the surface for the oxidation/reduction process and changes in the Auger line shapes of Ti in both cases, especially in the region corresponding to the LMV transition. As expected, this last result suggests changes in the Ti electron density of states due to the oxidation/reduction process.

To analyze the results in a more quantitative way, we depict in figure 2 the peak intensities corresponding to the  $Ti_{LMV}$  ( $\sim 418$  eV) and  $O_{KLL}$  ( $\sim 510$  eV) Auger transitions as a function of the electron bombardment time for both experiments already mentioned. The intensities were normalized to the  $Y(O_{KLL})$  initial yield of the  $TiO_2$  spectrum.

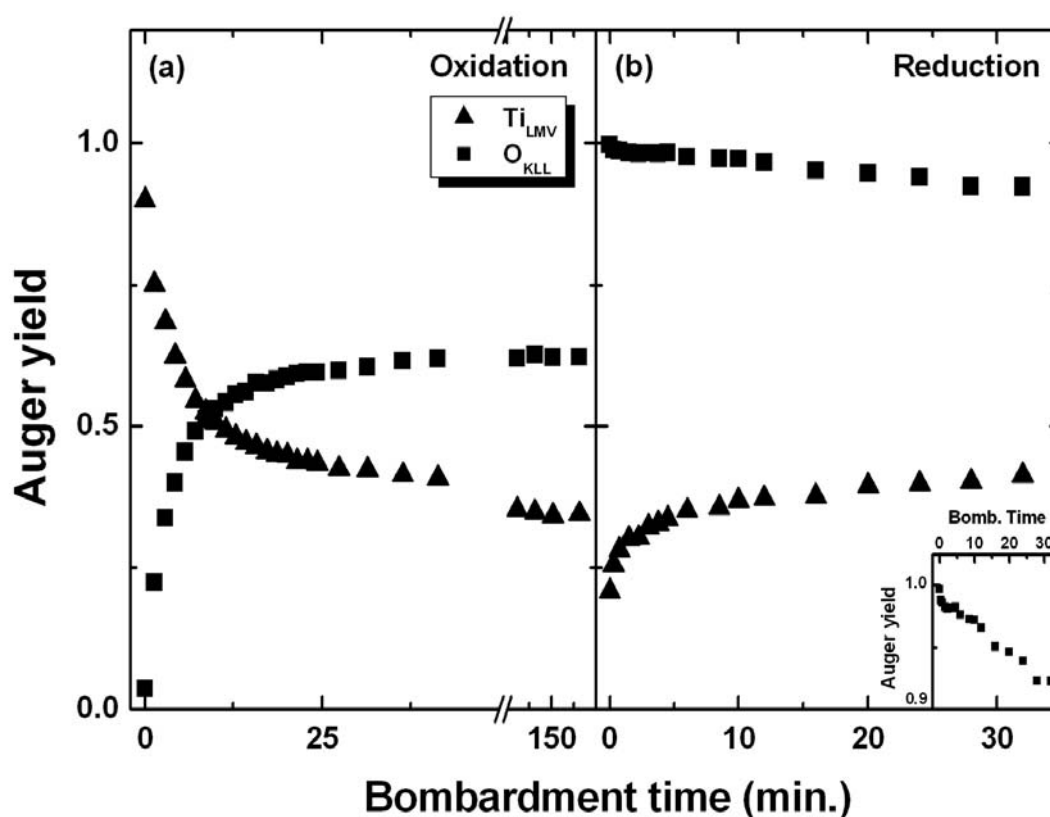


**Figure 2:** Evolution of the  $Ti_{LMV}$  ( $\blacktriangle$ ) and  $O_{KLL}$  ( $\blacksquare$ ) peak-to-peak Auger yields as a function of the electron bombardment time, for the metallic Ti oxidation (a) and  $TiO_2$  reduction (b) processes under electron irradiation. Inlet (2b): zoom of the  $O_{KLL}$  signal.

In figure 2a the  $Ti_{LMV}$  and  $O_{KLL}$  Auger yields show a typical oxidation behavior, with two clearly different evolution stages: an initial fast decrease/increase of the titanium/oxygen amount at the surface followed by a slowing down of the kinetics until a plateau is reached. In figure 2b we depict the results for the reduction process. Although a substantial change is observed for the  $Ti_{LMV}$  signal during the first 5 minutes of bombardment, i.e. a large monotonic increase, little modifications are

visible for the  $O_{KLL}$  signal in this scale. Thus, a zoom for the latter is shown in the inset of figure 2b. As we can see, the oxygen depletion begins as soon as the irradiation starts, showing a large monotonic decrease along the whole process.

A more detailed analysis can be performed based in the fact that only one of the main Ti Auger transitions involves valence electrons ( $Ti_{LMV}$ )<sup>(25)</sup>. Thus, it has been proposed that the ratio between both Ti Auger transitions yields,  $Y(Ti_{LMV})/Y(Ti_{LMM})$  hereinafter named as  $R_{VM}$ , can be used as a good indicator of the Ti oxidation state<sup>(26,27)</sup>. Moreover, comparing the evolution of this parameter with Factor Analysis results<sup>(19)</sup>, we showed that the evolution of the  $R_{VM}$  ratio can be used as a first indicator for a qualitative analysis.

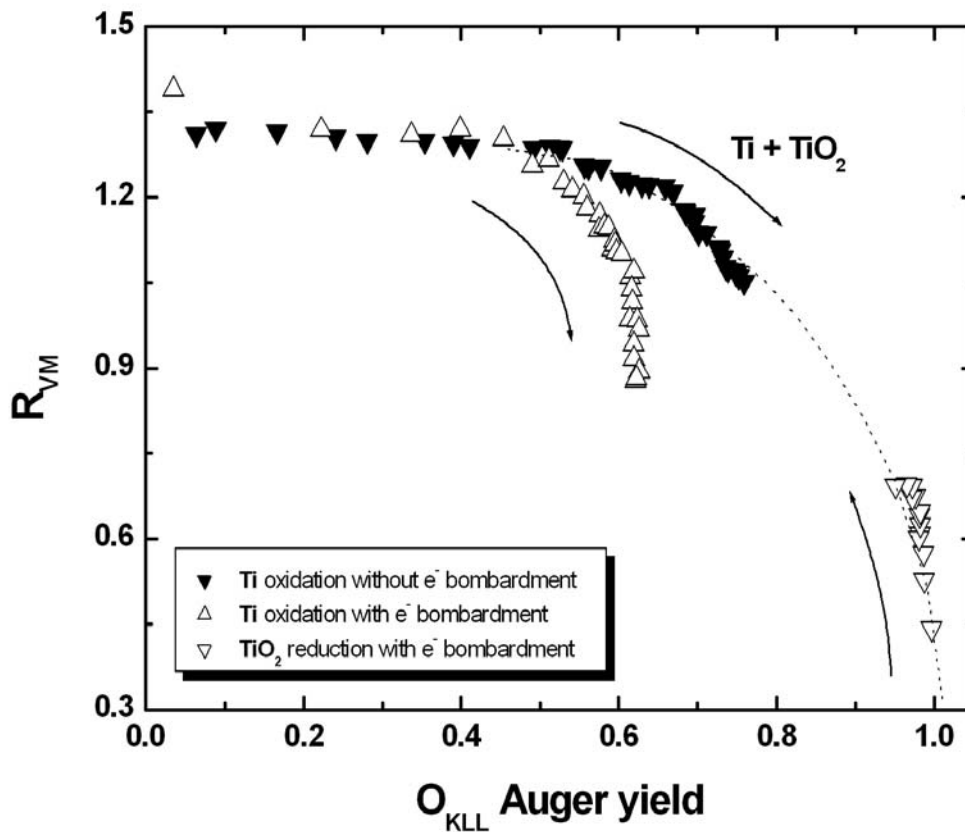


**Figure 3:** Evolution of the parameter  $R_{VM}$  as a function of the  $O_{KLL}$  Auger yield, for the metallic Ti oxidation ( $\Delta$ ) and  $TiO_2$  reduction ( $\nabla$ ) processes under electron irradiation. For comparison purposes, we added a curve obtained from measurements made keeping the electron bombardment to a minimum ( $\blacktriangledown$ )<sup>(19)</sup>.

In figure 3 we show the evolution of the  $R_{VM}$  ratio as a function of the oxygen Auger yield, for the experiments already mentioned. The arrows indicate the direction in which each experiment has been done. We can observe that the Ti oxidation state for the oxidation experiment strongly depends on the electron irradiation; in fact

changes in the  $R_{VM}$  ratio take place for lower  $O_{KLL}$  yields in comparison with measurements made keeping the electron bombardment to a minimum <sup>(19)</sup>. The same effect has been observed by decreasing/increasing the oxygen pressure/electron beam density for a given electron density/pressure. Thus, under electron irradiation we can get larger changes in the  $R_{VM}$  evolution for lower oxygen Auger yields <sup>(28)</sup>. These results can be explained based only in the oxygen enhanced diffusion induced by electron irradiation. In the case of the reduction experiment, the  $R_{VM}$  shows a monotonic increase originated in the electron transference to the Ti valence band (chemical reduction process), which is correlated with the monotonic decrease of the  $O_{KLL}$  yield along the process. The dot line, added in the figure as a guide to the eye, seems to suggest that the oxide reduction under electron irradiation might follow the same path as the Ti oxidation in a reversible way. As we will see this is not true, but in order to prove this fact we need to identify the different Ti compounds that appear along both experiment evolutions, by applying the Factor Analysis method <sup>(14)</sup> to the titanium Auger line shape evolutions.

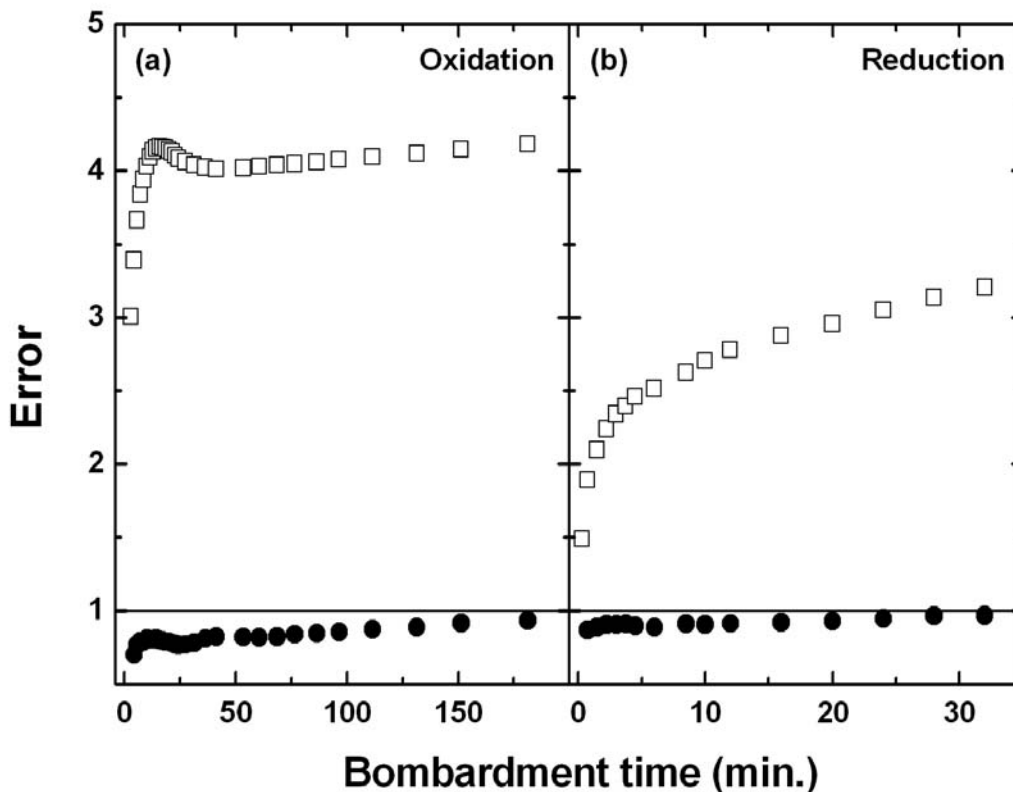


**Figure 4:** Evolution of the error attained in reproducing the data matrix as a function of the electron bombardment time considering one ( $\square$ ) and two ( $\bullet$ ) factors, for the metallic Ti oxidation (a) and  $TiO_2$  reduction (b) processes under electron irradiation. The horizontal line at unity corresponds to a calculated error equal to the EE.

In order to determine the number of independent components present in the oxidation and reduction processes, we apply the PCA in the sequential way<sup>(15,16,19)</sup>. In figure 4 we depict the evolution of the relative error attained in reproducing the experimental data, acquired along the irradiation process, using one and two factors. We found that both, the oxidation and reduction processes, can be described in terms of two independent components. Since metallic titanium and titanium dioxide are present as the starting surface component for the oxidation and reduction processes, respectively, under these particular analyzed conditions the results imply that only one Ti oxide is created by electron irradiation in both cases.

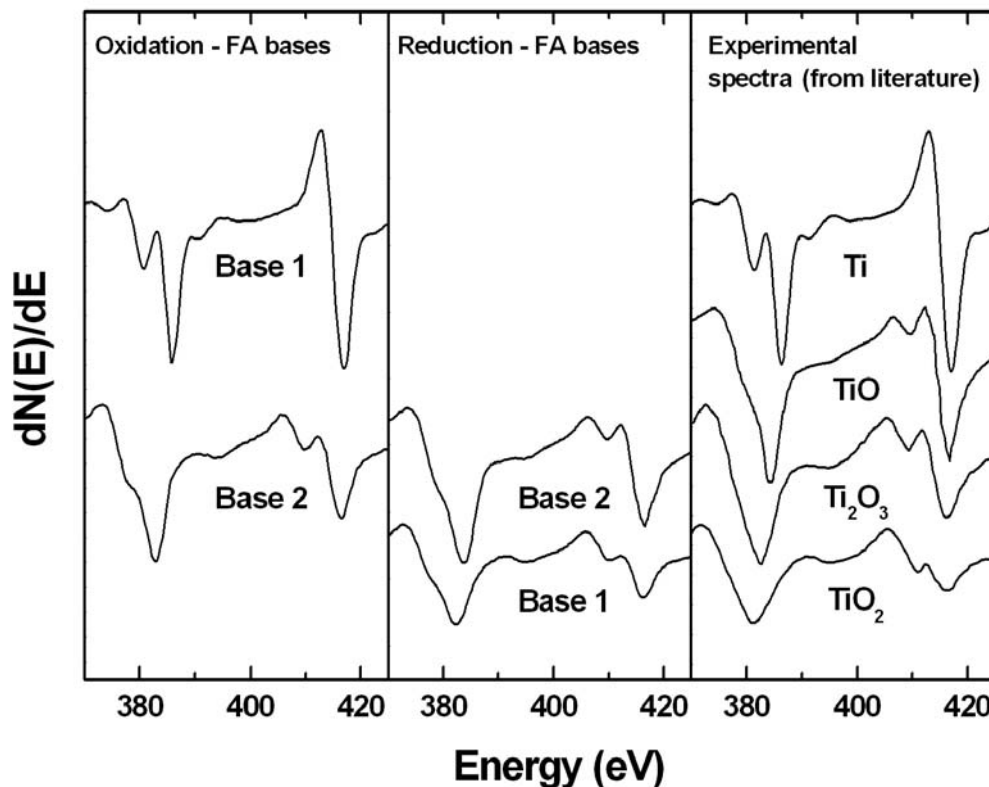


**Figure 5:** Auger spectra of the independent bases obtained after applying the TT method to the Ti spectra acquired along the electron stimulated oxidation of metallic Ti (left panel) and reduction of a  $\text{TiO}_2$  film under electron irradiation (centre panel). Experimental Auger spectra of  $\text{Ti}^{(20)}$  and its different compounds (right panel)<sup>(21,22)</sup>.

In figure 5 we compare the shape of the Auger spectra obtained through FA for the oxidation (left panel) and reduction (centre panel) processes with known experimental Auger spectra of  $\text{Ti}^{(20)}$  and different Ti oxides (right panel)<sup>(21,22,29,30)</sup>. The spectra ascribed to the first component (Base 1) obviously correspond to pure Ti for the oxidation process and  $\text{TiO}_2$  for the reduction process. The second component

spectrum seems to be the same for both experiments. A fingerprint procedure allows us to identify this second independent component as  $Ti_2O_3$  in both cases. The slight discrepancies observed among the bases coming from the different experiments, may point out the presence of small amounts of a third component. Within the FA capability of element identification, the oxidation and reduction processes are characterized by the appearance of only one Ti oxide, i.e.  $Ti_2O_3$ .

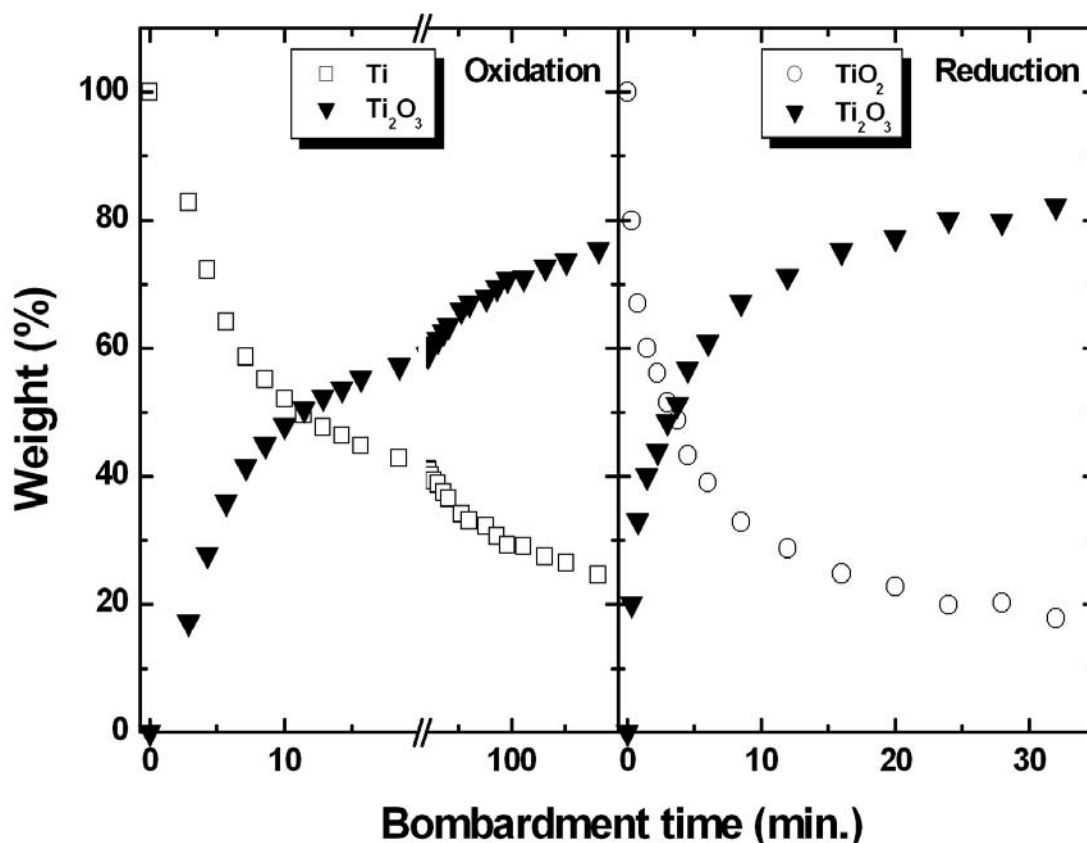


**Figure 6:** Evolution of the weights of the different titanium compounds obtained with the TT method as a function of the electron bombardment time, for the metallic Ti oxidation (left panel) and  $TiO_2$  reduction (right panel) processes under electron irradiation.

In figure 6 we show the evolution of the weights of each Auger spectra of the independent components in the total Auger line shape of the experimental spectra acquired along the complete irradiation processes under study. Both evolutions are characterized by a rapid metallic Ti depletion and  $TiO_2$  chemical reduction, giving place both to the formation of  $Ti_2O_3$ . Although, the oxide reaches a similar maximum weight in both experiments, it is clear that the reduction is a faster process. Another interesting issue to be noticed is that for both experiments the weights of  $Ti_2O_3$  reach a steady stage at a saturation value of about 80 %, which prevents the complete

disappearance of metallic Ti and TiO<sub>2</sub> in the oxidation and reduction processes, respectively. This last result can be explained as a consequence of the formation of little amounts of carbon at the surface, favored by the electron bombardment, which tends to stabilize the oxide preventing us to continue each process until a complete disappearance of metallic Ti or TiO<sub>2</sub> is obtained.

## CONCLUSIONS

We have characterized through Auger electron spectroscopy and Factor Analysis the titanium oxidation and titanium dioxide (Ti<sup>4+</sup>) chemical reduction processes under electron irradiation. We found that the electron bombardment affects the chemical reactions at the surface depending on the experimental environment. Thus, for the oxidation process we have a competition between the enhanced reaction kinetics, through the dissociation of oxygen molecules induced by the electron bombardment, and the stimulated desorption produced, for instance, through the Knotek-Feibelman process<sup>(28,31)</sup>. On the other hand, the stimulated desorption is the only process presents in the oxide reduction, previous to the C enhanced deposition. The measurable output in both cases is the appearance of a lower Ti oxidation state, i.e. Ti<sub>2</sub>O<sub>3</sub>.

## ACKNOWLEDGEMENT

This work has been partially supported by CONICET, ANPCyT and Universidad Nacional del Litoral through grants PIP 2553/99 and 5277, PICT 14730 and CAI+D 2000-6-6-62, respectively. One of us (R.B.) thanks the Universidad Nacional del Litoral for an undergraduate fellowship.

## REFERENCES

1. LINSEBIGLER, A.L.; LU, G.; YATES JR., J.T. **Chemical Reviews**, v. 95, p. 735, 1995.
2. KEISTER, F.Z. **Microelectronic Reliability**, v. 5, p. 95, 1966.
3. INTEMANN, A.; KOEMER, H.; KOCH, F. **Journal of the Electrochemical Society**, v. 140, p. 3215, 1993.
4. MULLER, U.; HAUERT, R. **Thin Solid Films**, v. 290-291, p. 323, 1996.
5. HANAWA, T.; OTA, M. **Applied Surface Science**, v. 55, p. 263, 1992.

6. SHEVELL, S. **Fundamental of Flight**. 2<sup>nd</sup> Ed., Prentice Hall, Englewoods Cliffs, New Jersey, 1989.
7. ESPINÓS, J.P.; FERNÁNDEZ, A.; GONZÁLEZ, A.R. **Surface Science**, v. 295, p. 402, 1993.
8. CHEN, S.; BOOTHROYD, C.B.; HUMPHREYS, C.J. **Applied Physics Letters**, v. 69, p. 170, 1996.
9. WATANABE, H.; FUJITA, J.; OCHIAI, Y.; MATSUI, S.; ICHIKAWA, M. **Japanese Journal of Applied Physics**, v. 34, p. 6950, 1995.
10. LANGHEINRICH, W.; SPANGENBERG, B.; BENEKING, H. **Journal of Vacuum Science and Technology B**, v. 10, p. 2868, 1992.
11. VERGARA, L.I.; VIDAL, R.; FERRÓN, J. **Applied Surface Science**, v. 229, p. 301, 2004.
12. PASSEGGI (JR.), M.C.G.; VAQUILA, I.; FERRÓN, J. **Surface and Interface Analysis**, v. 20, p. 761, 1993.
13. PASSEGGI (JR.), M.C.G.; VAQUILA, I.; FERRÓN, J. **Applied Surface Science**, v. 133, p. 65, 1998.
14. MALINOWSKI, E.; HOWERY, D. **Factor Analysis in Chemistry**. Wiley, New York, 1980.
15. VIDAL, R.A.; FERRÓN, J. **Applied Surface Science**, v. 31, p. 263, 1988.
16. STEREN, L.; VIDAL, R.A.; FERRÓN, J. **Applied Surface Science**, v. 29, p. 418, 1987.
17. PASSEGGI (JR.), M.C.G.; VERGARA, L.I.; MENDOZA, S.M.; FERRÓN, J. **Surface Science**, v. 507-510, p. 825, 2002.
18. VAQUILA, I.; PASSEGGI (JR.), M.C.G.; FERRÓN, J. **Physical Review B**, v. 55, p. 13925, 1997.
19. VAQUILA, I.; PASSEGGI (JR.), M.C.G.; FERRÓN, J. **Surface Science**, v. 292, p. L795, 1993.
20. DAVIS, L.E.; MAC DONALD, N.C.; PALMBERG, P.W.; RIACH, G.E.; WEBER, R.E. **Handbook of Auger Electron Spectroscopy**. Perkin-Elmer, Eden Prairie, 1978.
21. SOLOMON, J.S.; BAUN, W.L. **Surface Science**, v. 51, p. 228, 1975.
22. BERMUDEZ, V.M. **Journal of Vacuum Science and Technology**, v. 20, p. 51, 1982.

23. MITURA, E.; NIEDZIELSKA, A.; NIEDZIELSKI, P.; KLIMEK, L.; RYLSKI, A.; MITURA, S.; MOLL, J.; PIETRZYKOWSKI, W. *Diamond and Related Materials*, v. 5, p. 998, 1996.
24. FRAGE, N.; FROUMIN, N.; DARIEL, M.P. *Acta Materialia*, v. 50, p. 237, 2002.
25. SZALKOUSKI, F.J.; SOMORJAI, G. *Journal of Chemical Physics*, v. 56, p. 6097, 1972.
26. ROMAN, E.; SANCHEZ-AVEDILLO, M.; DE SEGOVIA, J.L. *Applied Physics A*, v. 35, p. 40, 1984.
27. RAV, C.N.; SARMA, D.D.; HEDGE, M.S. *Proceedings of the Royal Society of London A*, v. 370, p. 269, 1980.
28. BRASCA, R.; PASSEGGI (JR.), M.C.G.; FERRÓN, J. *Thin Solid Films*, in press, 2006.
29. GANDON, J.; JOUD, J.C. *Journal of the Less-Common Metals*, v. 69, p. 277, 1980.
30. VAQUILA, I.; PASSEGGI (JR.), M.C.G.; FERRÓN, J. *Applied Surface Science*, v. 93, p.247, 1996.
31. Knotek, M.L.; Feibelman, P.J. *Surface Science*, v. 90, p. 78, 1979.